JCI The Journal of Clinical Investigation

# Palmitoyl protein thioesterase-1 deficiency impairs synaptic vesicle recycling at nerve terminals, contributing to neuropathology in humans and mice

Sung-Jo Kim, Zhongjian Zhang, Chinmoy Sarkar, Pei-Chih Tsai, Yi-Ching Lee, Louis Dye, Anil B. Mukherjee

*J Clin Invest.* 2008;118(9):3075-3086. https://doi.org/10.1172/JCI33482.

**Research Article** **Neuroscience**

Neuronal ceroid lipofuscinoses represent the most common childhood neurodegenerative storage disorders. Infantile neuronal ceroid lipofuscinosis (INCL) is caused by palmitoyl protein thioesterase-1 (PPT1) deficiency. Although INCL patients show signs of abnormal neurotransmission, manifested by myoclonus and seizures, the molecular mechanisms by which PPT1 deficiency causes this abnormality remain obscure. Neurotransmission relies on repeated cycles of exo- and endocytosis of the synaptic vesicles (SVs), in which several palmitoylated proteins play critical roles. These proteins facilitate membrane fusion, which is required for neurotransmitter exocytosis, recycling of the fused SV membrane components, and regeneration of fresh vesicles. However, palmitoylated proteins require depalmitoylation for recycling. Using postmortem brain tissues from an INCL patient and tissue from the PPT1-knockout (PPT1-KO) mice that mimic INCL, we report here that PPT1 deficiency caused persistent membrane anchorage of the palmitoylated SV proteins, which hindered the recycling of the vesicle components that normally fuse with the presynaptic plasma membrane during SV exocytosis. Thus, the regeneration of fresh SVs, essential for maintaining the SV pool size at the synapses, was impaired, leading to a progressive loss of readily releasable SVs and abnormal neurotransmission. This abnormality may contribute to INCL neuropathology.



# Palmitoyl protein thioesterase-1 deficiency impairs synaptic vesicle recycling at nerve terminals, contributing to neuropathology in humans and mice

Sung-Jo Kim,[1] Zhongjian Zhang,[1] Chinmoy Sarkar,[1] Pei-Chih Tsai,[1] Yi-Ching Lee,[1] Louis Dye,[2] and Anil B. Mukherjee[1]

[1]Section on Developmental Genetics, Heritable Disorders Branch, and [2]Microscopy and Imaging Core, National Institute of Child Health and Human Development, NIH, Bethesda, Maryland, USA.

**Neuronal ceroid lipofuscinoses represent the most common childhood neurodegenerative storage disorders. Infantile neuronal ceroid lipofuscinosis (INCL) is caused by palmitoyl protein thioesterase-1 (PPT1) deficiency. Although INCL patients show signs of abnormal neurotransmission, manifested by myoclonus and seizures, the molecular mechanisms by which PPT1 deficiency causes this abnormality remain obscure. Neurotransmission relies on repeated cycles of exo- and endocytosis of the synaptic vesicles (SVs), in which several palmitoylated proteins play critical roles. These proteins facilitate membrane fusion, which is required for neurotransmitter exocytosis, recycling of the fused SV membrane components, and regeneration of fresh vesicles. However, palmitoylated proteins require depalmitoylation for recycling. Using postmortem brain tissues from an INCL patient and tissue from the PPT1-knockout (PPT1-KO) mice that mimic INCL, we report here that PPT1 deficiency caused persistent membrane anchorage of the palmitoylated SV proteins, which hindered the recycling of the vesicle components that normally fuse with the presynaptic plasma membrane during SV exocytosis. Thus, the regeneration of fresh SVs, essential for maintaining the SV pool size at the synapses, was impaired, leading to a progressive loss of readily releasable SVs and abnormal neurotransmission. This abnormality may contribute to INCL neuropathology.**

## Introduction

In the nervous system, many proteins undergo palmitoylation (*S*-acylation), a posttranslational modification in which a 16-carbon fatty acid, palmitate, is attached to specific cysteine residues in polypeptides via thioester linkages (reviewed in refs. 1–3). Palmitoylation plays critical roles in diverse biological functions, including membrane anchorage, vesicular transport, signal transduction, and the maintenance of cellular architecture (1–3). There are at least 100 proteins known to date that are palmitoylated (1), and this list is growing. Moreover, repeated cycles of palmitoylation and depalmitoylation have been suggested to regulate the distribution of proteins between the membrane and the cytoplasm and/or between subdomains of the plasma membrane that modulate the coupling of specific signaling proteins to cell surface receptors or intracellular effectors (1–3).

The characterization of palmitoyl acyltransferases (4), which catalyze the linking of palmitate with specific cysteine residues in polypeptides via thioester linkage, and palmitoyl protein thioesterase-1 (PPT1) (5), a depalmitoylating enzyme that cleaves thioester linkages, removing the palmitate residues from the *S*-acylated proteins, advanced our knowledge of the importance of dynamic protein palmitoylation in biological processes (1–3). The molecular cloning and characterization of the PPT1 cDNA and the gene as well as its chromosomal localization (6) facilitated the discovery that inactivating mutations in the *PPT1* gene causes infantile neuronal ceroid lipofuscinosis (INCL) (7), a devastating childhood neurodegenerative storage disorder for which there is no effective treatment. INCL belongs to a group of the most common (1 in 12,500 births) hereditary neurodegenerative storage disorders known as neuronal ceroid lipofuscinoses, or more commonly, Batten disease (8–12). Children afflicted with INCL are normal at birth, but by 2 years of age they undergo complete retinal degeneration leading to blindness, and by age 4 they fail to manifest any brain activity. These children remain in a vegetative state for 8–10 more years before death (8–12). Early in the disease course, INCL patients develop myoclonic jerks and seizures, which are some of the clinical manifestations of abnormal neuronal communication (13). Disruption of neuronal communication may also contribute to neurodegeneration. However, the molecular mechanism(s) by which PPT1 deficiency leads to abnormal neurotransmission and neurodegeneration remains poorly understood. Consequently, there is no effective treatment for INCL, and this disease remains uniformly fatal. Understanding the molecular mechanism(s) of INCL pathogenesis may facilitate the development of novel therapeutic approaches.

Recent reports indicate that neuronal communication relies on repeated cycles of exo- and endocytosis of the neurotransmitter-laden synaptic vesicles (SVs) at the nerve terminals (14–17). The fusion of the SV membrane with the presynaptic plasma membrane

**Nonstandard abbreviations used:** GAD65, glutamic acid decarboxylase 65; INCL, infantile neuronal ceroid lipofuscinosis; PPT1, palmitoyl protein thioesterase-1; SNAP25, synaptosomal-associated protein, 25 kDa; SV, synaptic vesicle; SYTI, synaptotagmin I; VAMP2, synaptobrevin 2.

**Conflict of interest:** The authors have declared that no conflict of interest exists.

**Citation for this article:** *J. Clin. Invest.* **118**:3075–3086 (2008). doi:10.1172/JCI33482.

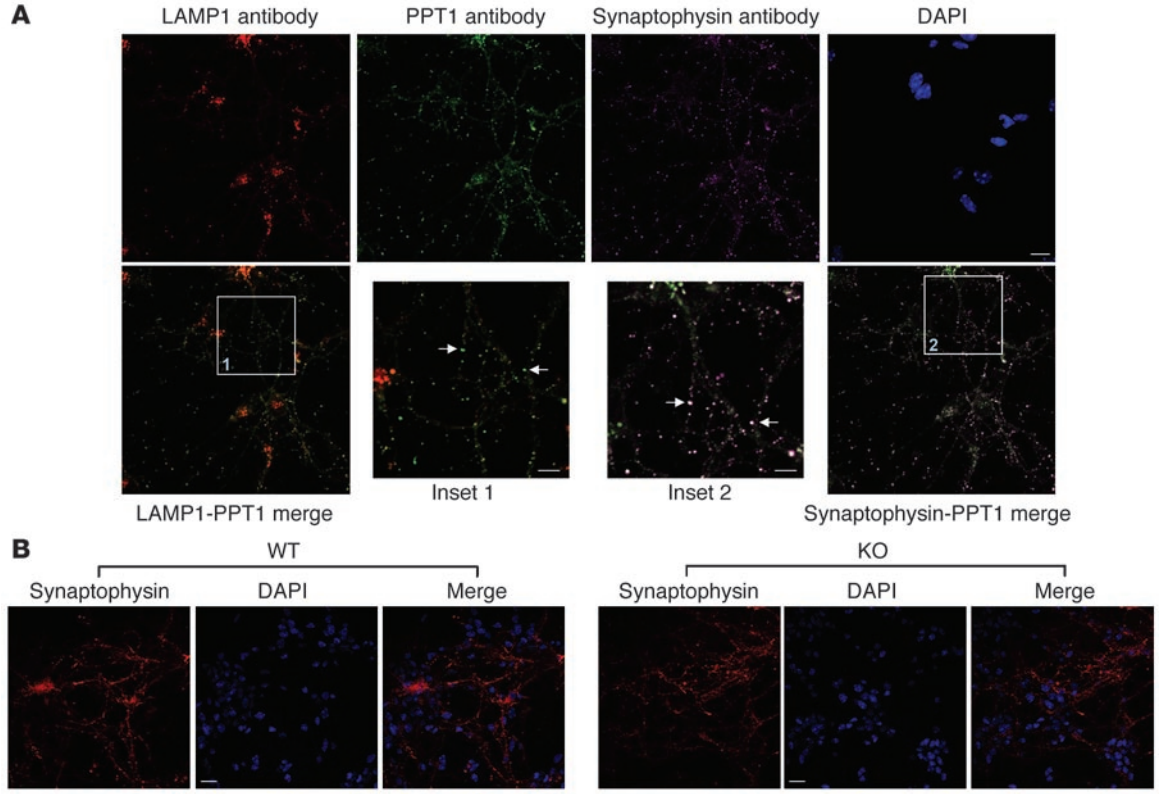


**Figure 1**
Immunolocalization of PPT1 in primary neuron cultures. (**A**) Confocal microscopic detection of PPT1 (green), LAMP1 (red), and synaptophysin (purple) in the WT littermate neurons. Nuclei were stained by DAPI. Scale bars: 20 μm. While the PPT1 immunoreactivity colocalized with LAMP1 in the main cell body, the 2 arrows in the merged image of LAMP1 and PPT1 show that in the axon, PPT1 and LAMP1 immunoreactivities are not colocalized (inset 1), suggesting the extralysosomal presence of PPT1. Extralysosomal PPT1 immunoreactivity also colocalized with synaptophysin (inset 2). (**B**) Confocal microscopic image of synaptophysin (red). Note that both the PPT1-KO and WT neurons had virtually identical neuronal projections. Nuclei were stained with DAPI (blue). Scale bars: 50 μm.

facilitates neurotransmitter exocytosis. This event is followed by the detachment of the vesicle components from the presynaptic plasma membrane and the recycling of these components, including several proteins that play critical roles in membrane fusion, exocytosis, and regeneration of fresh vesicles. The freshly formed SVs then replenish the SV pool at the neuronal synapses for further rounds of use (14–17). The SV-associated SNARE proteins, such as synaptobrevin 2 (VAMP2), syntaxin 1, and synaptosomal-associated protein, 25 kDa (SNAP25) (16-19), play critical roles in mediating anchorage and fusion of the vesicles with the presynaptic plasma membrane, essential for SV exocytosis and neurotransmitter release (19, 20). Among the SNARE proteins, VAMP2 (21) and SNAP25 (22) undergo palmitoylation, while syntaxin 1 is not palmitoylated. However, syntaxin 1 binds SNAP25 (23), which may act as a scaffold for syntaxin 1 to gain membrane access. In addition, several non-SNARE proteins such as synaptotagmin (SYTI) (24) and glutamic acid decarboxylase 65 (GAD65) are also palmitoylated (25–27) and participate in the SV recycling process.

Although the protein palmitoylation plays critical roles in neurotransmitter release and the maintenance of synaptic strength (28), the palmitoylated proteins associated with the SVs must undergo depalmitoylation in order to be detached from the membrane, recycled, and/or degraded (1–3). PPT1 (5) catalyzes the cleavage of thioester linkages in membrane-anchored *S*-acylated proteins, allowing them to detach from the membrane. Thus, we hypothesized that in order for the *S*-acylated SV proteins to undergo depalmitoylation, PPT1 must be present in the presynaptic compartment. However, PPT1 is known to be a lysosomal enzyme (29, 30), and the reports of its localization in the presynaptic compartment (synaptosomes and SVs) of cultured neurons remain controversial because these studies were conducted using neurons in which PPT1 was overexpressed by viral transfection (31–33). Thus, to determine whether PPT1 has a role in neuronal communication, it is necessary to establish whether this enzyme can be localized in the presynaptic compartment (i.e., synaptosomes and/or the SVs) under physiological conditions.

In the present study, we first sought to determine whether, under physiological conditions, PPT1 is detectable in the presynaptic compartment of neurons. We then examined whether the lack of PPT1 adversely affects the trafficking and/or recycling of SV proteins, VAMP2, SNAP25, syntaxin 1, SYTI, and GAD65, which are known to play critical roles in the exocytosis, recycling, and the regeneration of SVs. Here we report that, under physiological conditions, PPT1 is localized in the synaptosomes and SVs and that its deficiency causes abnormal and persistent membrane association of the said SV proteins. We propose that this abnormality leads to the disruption of SV recycling and prevents the regeneration of fresh vesicles. Consequently, the progressive

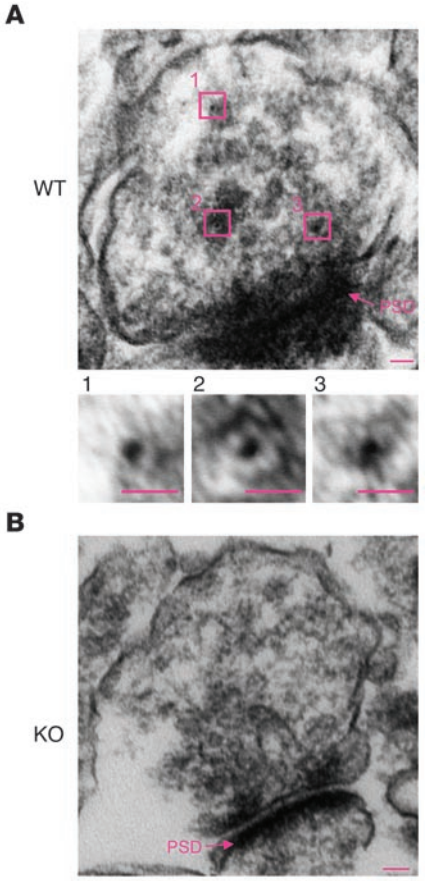


**Figure 2**
Immunoelectron microscopic detection of PPT1 protein in the synaptosomes of WT mouse brain. (**A**) Immunogold staining for PPT1 within the synaptosome. Insets show the magnified views of the gold particles. (**B**) No PPT1 immunoreactivity was detected in the PPT1-KO brain. PSD, postsynaptic density. Scale bars: 100 nm; 50 nm (insets).

decline in the total as well as the readily releasable SV pool size occurs at the neuronal synapses that impair neurotransmission, contributing to INCL neuropathology.

## Results

*PPT1 is present in synaptosomes and SVs under physiological conditions.* To determine the presence of PPT1 in synaptosomes and SVs, we first examined cultured neurons from cerebral cortex or from those differentiated from neurospheres derived from the PPT1-KO mice (34) that mimic INCL (35) and from their WT littermates. These neurons were used for immunocytochemical analyses by confocal microscopy to determine whether PPT1 immunoreactivity colocalizes with lysosomal marker protein LAMP1 and the SV marker protein, synaptophysin. The results show that, while the PPT1 immunoreactivity predominantly colocalizes with LAMP1, a low level of this immunoreactivity does not appear to colocalize with LAMP1 (Figure 1A). However, this low level of PPT1 immunoreactivity clearly colocalizes with that of synaptophysin (Figure 1A). Taken together, these results suggest that at least a small fraction of PPT1 immunoreactivity is localized in the presynaptic compartment and is most likely associated with the synaptosomes and SVs. We used the PPT1-KO neurons as a control, and these neurons did not show any evidence of PPT1-specific immunoreactivity (data not shown). We also analyzed the cultured PPT1-KO and WT neurons morphologically for projections and synapses after staining them with synaptophysin antibody, and the results show that there is virtually no morphological difference between the WT and the PPT1-deficient neurons (Figure 1B).

To further confirm the above results, we analyzed the brain tissues from the PPT1-KO mice and those of their WT littermates by immunoelectron microscopy, using monospecific PPT1 antibody and immunogold-labeled secondary antibody. The results confirm that PPT1 immunoreactivity is indeed localized in the presynaptic compartment (i.e., synaptosomes and SVs) in the brains of WT mice (Figure 2A), but not in that of their PPT1-KO littermates (Figure 2B). Taken together, these results strongly suggest that, under in vivo physiological conditions, PPT1 is present in the synaptosomes and on the SVs.

*Reduced levels of SV proteins in the soluble fractions of the INCL brain.* The SNARE proteins VAMP2, SNAP25, and syntaxin 1 are the driving force for membrane fusion and SV exocytosis at the neuronal synapses (14–18, 36, 37). Among these, VAMP2 as well as SNAP25 undergo palmitoylation and play critical roles in SV fusion with presynaptic plasma membrane for exocytosis (19), effecting neurotransmitter release (14, 38). Moreover, VAMP2 also plays a role in rapid endocytosis of vesicle constituents to regenerate fresh SVs (39) for further rounds of use. While syntaxin 1 does not undergo palmitoylation, it interacts with SNAP25 and may become associated with the SV membrane. Further, these proteins also participate in the recycling and regeneration of the fresh SVs following exocytosis, essential for replenishing the SV pool at the synaptic terminal (15, 16, 40). However, a precondition for recycling of *S*-acylated proteins is depalmitoylation, which facilitates the removal of the palmitate residues so that the protein can detach from the membrane to which it is anchored and recycle. Therefore, we rationalized that PPT1 deficiency may cause persistent membrane anchorage of these proteins and impair SV recycling. Accordingly, we first determined the levels of several SV proteins in the soluble fractions of homogenates of postmortem brain tissues from an INCL patient and in those of an age-matched normal control by western blot analysis. We initially chose the SNARE proteins VAMP2, SNAP25, and syntaxin 1, as these proteins play critical roles in the fusion of SVs to the presynaptic plasma membrane during exocytosis (27, 41). The results show that, compared with the normal control, the levels of VAMP2 (Figure 3A), SNAP25 (Figure 3B), and syntaxin 1 (Figure 3C) in the INCL brain lysates are strikingly lower. Similarly, the levels of SYTI and GAD65 (Supplemental Methods; supplemental material available online with this article; doi:10.1172/JCI33482DS1) are also significantly lower in the INCL brain lysates compared with those of the normal control (Supplemental Figure 1, A and B). These results suggest that PPT1 deficiency leads to abnormally low levels of soluble SV proteins that are known to undergo palmitoylation and are critical for fusion, exocytosis, recycling, and regeneration of fresh SVs.

*Decreased SV protein levels in the soluble fractions of the PPT1-KO brain lysates.* To confirm the results described above, we used the lysates of brain tissues from 1-, 3-, and 6-month-old PPT1-KO mice that mimic INCL as well as those of their WT littermates and analyzed the soluble proteins by western blot. The results show that, compared with the WT littermates, VAMP2 (Figure 3D), SNAP25 (Figure 3E), and syntaxin 1 (Figure 3F) levels in the PPT1-KO brain

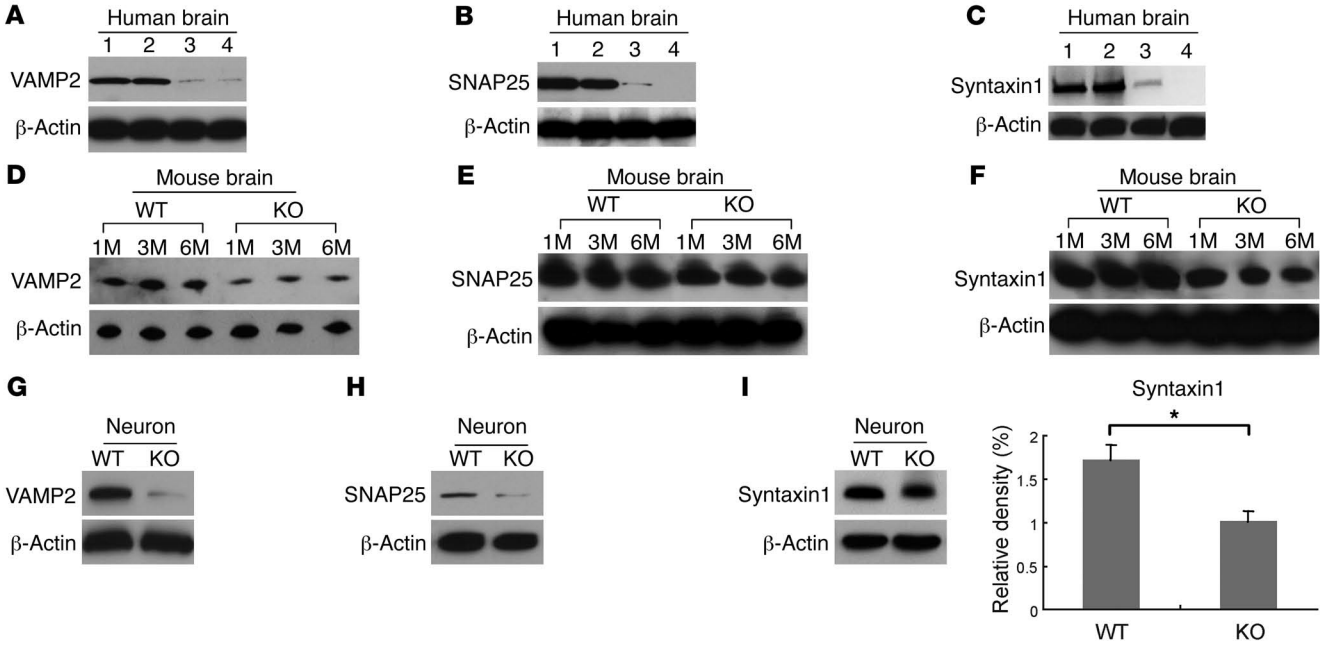


**Figure 3**

Levels of SV proteins in the soluble fractions of homogenates of the brain tissues and cultured neurons. (**A**–**C**) Western blot analyses of postmortem brain tissue lysates of a normal control and an INCL patient. (**A**) VAMP2, (**B**) SNAP25, (**C**) syntaxin 1. Lane 1, normal hippocampus; lane 2, normal cortex; lane 3, INCL hippocampus; lane 4, INCL cortex. (**D**–**F**) Western blot analyses of brain lysates from WT mice and their PPT1-KO littermates. (**D**) VAMP2, (**E**) SNAP25, (**F**) syntaxin 1. 1M, 1 month; 3M, 3 months; 6M, 6 months. Note PPT1 deficiency caused decreased levels of SV proteins in the soluble fractions. (**G**–**H**) Western blot analyses of the soluble fractions of cultured neurons from the WT and PPT1-KO neuron lysates. (**G**) VAMP2, (**H**) SNAP25, and (**I**) syntaxin 1. Densitometric analysis of syntaxin 1 is shown on the right side of **I**. Data are mean ± SD ($n$ = 3).

homogenates are appreciably lower. As previously indicated, although syntaxin 1 does not undergo palmitoylation, it binds SNAP25 and follows a pattern similar to that of SNAP25 in western blot analysis (Supplemental Methods). The levels of SYTI and GAD65 were also virtually identical to those of VAMP2, SNAP25, and syntaxin 1 (Supplemental Figure 1, C and D). These results prompted us to examine whether PPT1 deficiency downregulates the transcription of these genes. Accordingly, using total RNA from the cerebral cortex of the PPT1-KO mice and their WT littermates, we determined the mRNA levels of these genes by real time RT-PCR (Supplemental Methods and Supplemental Table 1). The results show that there is virtually no difference in the mRNA levels of those genes in the brain tissues of PPT1-KO mice and their WT littermates (Supplemental Figure 2, A–E). These results suggest that the effect of PPT1 deficiency is at the protein level and not at the mRNA level.

*Soluble fractions of PPT1-deficient neurons contain reduced levels of SV proteins.* To further confirm the results described, we resolved the soluble proteins from the lysates of cultured neurons differentiated from WT and PPT1-KO neurospheres by SDS-PAGE and western blot analysis. Again, the results confirm that, compared with the soluble fractions of the lysates of WT neurons, those of the PPT1-KO neurons contain appreciably lower levels of VAMP2 (Figure 3G), SNAP25 (Figure 3H), and syntaxin 1 (Figure 3I). Similar patterns were also observed for SYTI and GAD65 (Supplemental Figure 3, A and B). Taken together, these results show that PPT1 deficiency causes an abnormally low level of SV proteins in the soluble fractions of the postmortem brain tissues from an INCL patient and PPT1-KO mice as well as in the lysates of PPT1-deficient cultured neurons. Taken together, these results raised the possibility that lack of PPT1 may cause the *S*-acylated proteins to remain anchored to the membrane, thereby reducing the levels in the soluble fractions.

*Abnormal trafficking of palmitoylated SV proteins in PPT1-KO neurons.* To determine whether PPT1 deficiency causes abnormal trafficking and persistent membrane retention of palmitoylated SV proteins, we performed western blot analysis of 2 representative SV proteins, VAMP2 and SNAP25, from both the soluble and membrane fractions of cultured WT and PPT1-KO neurons. We chose these 2 proteins because they are SNARE proteins critical for SV membrane fusion with the presynaptic membrane and VAMP2 facilitates rapid endocytosis (39), enabling the regeneration of fresh SVs. Our results show that in the soluble fractions of WT neurons, the VAMP2 (Figure 4A) and SNAP25 (Figure 4B) protein bands are clearly detectable, while the protein bands in the PPT1-KO neurons are markedly less intense. Most interestingly, while the levels of these proteins in the membrane and in the soluble fractions of the WT neurons are very similar, those from the membrane fractions of the PPT1-KO neurons are markedly higher compared with those of the soluble fractions. To determine whether a pattern of localization of SV proteins could be recognized at the cellular level, we examined the cultured PPT1-KO and WT neurons by histochemical analysis using antibodies against VAMP2 or SNAP25. The results show that in the PPT1-KO neurons, VAMP2 (Figure 4C) and SNAP25 (Figure 4D) immunoreactivities appear to localize more prominently in the synapses. These results suggest that, due to the PPT1 deficiency, palmitoylated SV proteins are disproportionately and persistently sorted to the membranes, especially to the synaptic membranes.

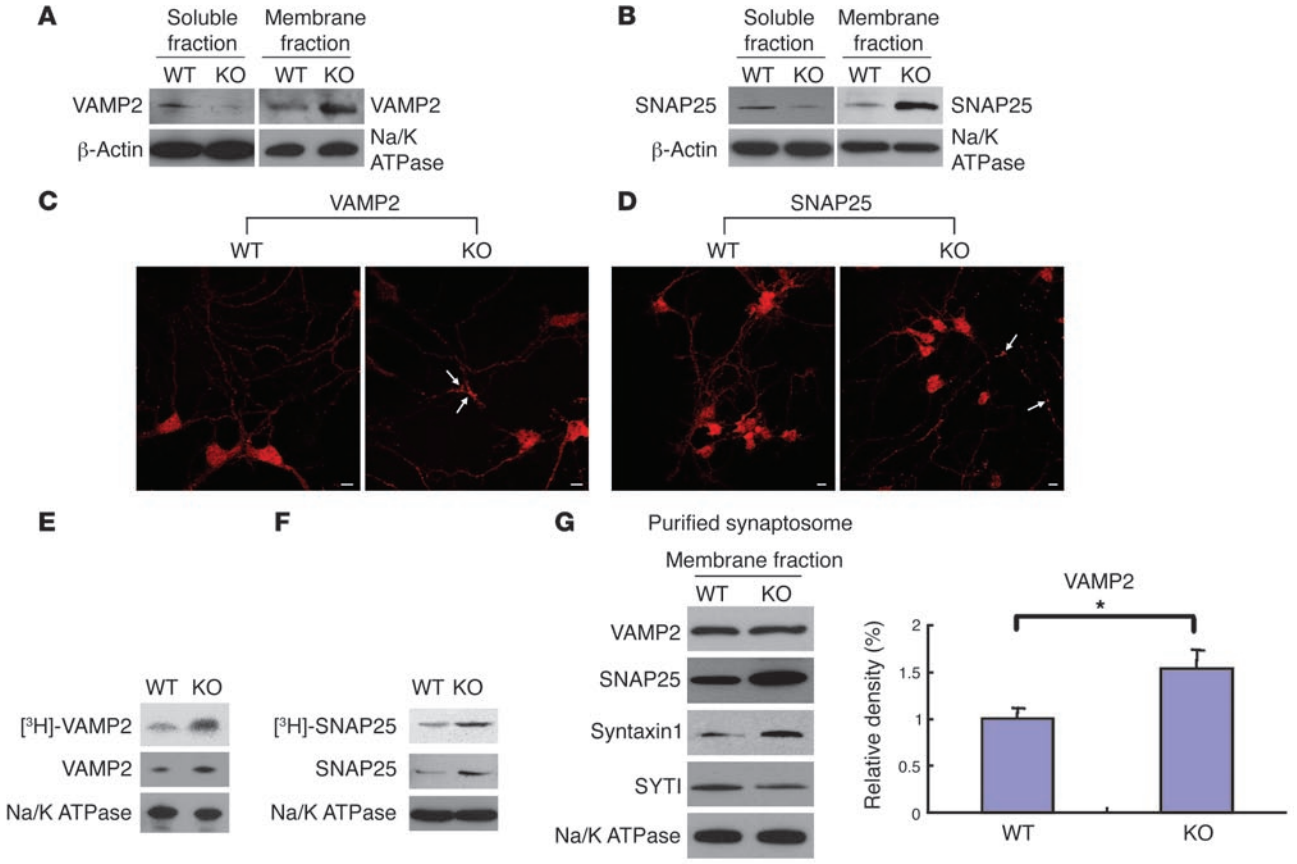


**Figure 4**
Persistent membrane association of SV proteins from the cortex of PPT1-KO mice. Western blot analysis of (**A**) VAMP2 and (**B**) SNAP25 in WT and PPT1-KO mice. β-Actin was used as the loading standard for soluble proteins and Na/K ATPase for the membrane proteins. Confocal microscopic analysis of (**C**) VAMP2 and (**D**) SNAP25 immunoreactivity in the PPT1-KO and WT cultured neurons. Scale bars: 20 μm. Newly palmitoylated VAMP2 (**E**) and SNAP25 (**F**) in cultured neurons differentiated from WT and PPT1-KO neurospheres. Na/K ATPase was used as the membrane fraction loading control. (**G**) Western blot analysis of purified synaptosomal/SV membrane fractions of the cortical tissues from the PPT1-KO mice and their WT littermates. Na/K ATPase, which is not a palmitoylated protein, was used as the membrane protein loading standard. Densitometric analysis of VAMP2 is shown on the right side of **G**. Error bars indicate SD ($n$ = 3).

*Lack of PPT1 causes increased membrane sorting of freshly palmitoylated proteins*. To determine whether PPT1 deficiency causes increased membrane sorting and retention of freshly palmitoylated VAMP2 and SNAP25, we first labeled the cells with [$^3$H]-palmitate and immunoprecipitated these proteins in the membrane fractions using their respective antibodies. The immunoprecipitates were resolved by SDS-PAGE and western blot analysis. The results show that compared with the membrane-fractions of the WT neurons, those of the PPT1-KO neurons contained appreciably more [$^3$H]-palmitate–labeled VAMP2 (Figure 4E) and SNAP25 (Figure 4F) proteins. These results demonstrate that due to the lack of PPT1, SV proteins in PPT1-KO neurons fail to detach from the membrane and may impair recycling and regeneration of fresh SVs.

*SV protein levels in purified synaptosomes from PPT1-KO and WT mice*. So far, we have observed the patterns of various SV proteins in the total lysates of postmortem INCL brain tissues as well as those in the total membrane fractions and compared the results with those of the normal control. In addition, we analyzed the brain tissues from the PPT1-KO mice and those of their WT littermates. However, we realized that the protein patterns from total brain lysates may not reflect those in the synaptosomes and SVs. We therefore purified the synaptosomes from the cerebral cortex of the PPT1-KO mice and their WT littermates. We then analyzed the proteins from the synaptosomal preparations by western blot analysis. The results showed that compared with the membrane fractions of the WT synaptosomes, those of the PPT1-KO synaptosomes appeared to contain a slightly higher level of VAMP2 but markedly elevated levels of SNAP25 and syntaxin 1 (Figure 4G). Similar patterns were also observed for SYTI and GAD65 (Supplemental Figure 4A). Synaptophysin was used as the SV marker, and Na/K ATPase was used to standardize membrane protein loading. Our results showed that the pattern of sorting and retention of these proteins, observed in the membrane fractions of total lysates of brain tissues, remained unaltered in purified synaptosome preparations. These results are consistent with our general conclusion that PPT1 deficiency leads to abnormal sorting and retention of palmitoylated SV proteins to the membrane, which most likely disrupts the recycling as well as regeneration of fresh vesicles, causing a decline in the SV pool size.

*Abnormal membrane sorting of SV proteins is corrected by PPT1*. To determine whether the abnormal pattern of membrane sorting observed in the PPT1-deficient neurons is correctable by PPT1,

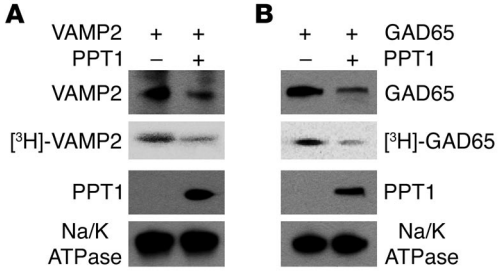


**Figure 5**
Correction of persistent membrane association of SV proteins in PPT1-deficient cells by PPT1 cDNA transfection. We transfected PPT1-KO astrocytes/glial cells with either VAMP2 (**A**) or GAD65 (**B**) cDNA constructs. Some of the transfected VAMP2 and GAD65 cultures were further transfected with PPT1 cDNA and labeled with [$^3$H]-palmitate. The proteins from the membrane fractions were resolved and analyzed by SDS-PAGE, western blot, and autoradiography. The right lanes of each panel represent PPT1 cotransfected cells. Note decreasing levels of membrane-associated VAMP2 and GAD65 in PPT1-KO cells transfected with PPT1. Na/K ATPase was used as the membrane fraction loading standard.

we transfected PPT1-deficient astrocytes with VAMP2 or GAD65 cDNA constructs. Some of these cells were double transfected with a PPT1 cDNA construct. The cells were then labeled with [$^3$H]-palmitate, and the proteins in the membrane fractions were resolved by immunoprecipitation, SDS-PAGE, western blotting, and autoradiography. The results show that, while in the absence of PPT1 high levels of VAMP2 (Figure 5A) and GAD65 (Figure 5B) are associated with the membrane fraction, these levels are markedly reduced in cells double transfected with PPT1. These results suggest that the abnormal membrane sorting patterns observed in the brain tissues of the INCL patient and the PPT1-KO mice most likely result from the absence of PPT1, indicating that the SV proteins considered in this study may be some of the substrates of PPT1. This, however, requires further confirmation.

*PPT1-KO mice show progressive decline of the SV pool size.* Since abnormal membrane sorting and retention of VAMP2, SNAP25, syntaxin 1, SYTI, and GAD65 may impair regeneration of fresh vesicles, we sought to determine whether such abnormality may reduce the total SV pool size in the PPT1-KO neurons. Accordingly, we used the cortical tissues from both PPT1-KO and WT littermates at 1, 3, and 6 months of age and analyzed them by transmission electron microscopy. The results show that compared with the brain tissues of the WT mice, those of the PPT1-KO littermates show a decline in the total SV pool (Figure 6A), which is most appreciable from 6 months of age, although the ratio of docked to total pool remained virtually unaltered. Quantitative analysis of the SVs in the PPT1-KO and WT brain show that, while at 1 and 3 months of age there is no significant change in the total SV pool, at 6 months of age a significant ($P < 0.0001$) reduction in the total SV pool size occurs in cortical neurons of the PPT1-KO mice, although the ratio of docked vesicle to total vesicle pool is not markedly affected (Figure 6A). Coincidentally, at this age the PPT1-KO mice also begin to manifest signs of neurological impairment (34, 35). These results are consistent with the notion that lack of PPT1 causes abnormal sorting and retention of the proteins, which are critical for SV recycling, thereby disrupting the recycling and regeneration of fresh SVs in the synaptic terminal and causing a progressive decline in the total SV pool size.

*Readily releasable SV pool is markedly reduced in PPT1-KO neurons.* In the presynaptic compartment, SVs are classified into several pools defined by their morphological and physiological characteristics (40). For example, subsets of vesicles that interact with the presynaptic membrane are called the "readily releasable (active) pool," and the exocytosis of these SVs can be elicited by membrane depolarization with high-molarity KCl (42). There are also the "recycling pool," the "reserve pool," and empty vesicles that are newly recruited by endocytosis following neurotransmitter release (40).

The SVs in the presynaptic compartment are clustered together and, upon arrival of an action potential, fuse with the presynaptic plasma membrane for neurotransmitter release by exocytosis. However, the vesicle components, including the proteins, must recycle to regenerate fresh vesicles, replenishing the SV pool for further rounds of use (40). Fluorescent markers, especially styryl dyes such as FM1-43FX, have been successfully used to follow exo- and endocytic events in many cell types including neurons (43). We rationalized that the observed age-dependent reduction of the SV pool size in the PPT1-KO brain may be the result of the inability of the exocytosed SVs to recycle because of their persistent anchorage to, and retention by, the presynaptic plasma membrane. Thus, the readily releasable SV pool size may gradually decrease with time, causing the total SV pool size to decline. Accordingly, we loaded the WT and PPT1-KO neurons, differentiated from neurospheres, with FM1-43FX and determined the release of fluorescence with the chemical stimulus for depolarization of the cells. Our results showed that compared with the WT controls, the PPT1-KO neurons had a significantly lower level of FM1-43FX fluorescence ($P < 0.0001$; Figure 6B), clearly indicating a decline in the number of readily releasable (active) SVs. The quantitative analysis of FM1-43FX fluorescence indicated a sharp decline in the readily releasable pool size (Figure 6B). We also repeated these experiments using cultured cortical neurons from the PPT1-KO mice and their WT littermates (see Supplemental Methods), and the results were virtually identical to those obtained from neurons differentiated from cultured neurospheres (Supplemental Figure 4B). Taken together, these results demonstrate that PPT1 deficiency leads to persistent membrane association of *S*-acylated SV proteins, which are critical for SV regeneration at the nerve terminals, and causes progressive decline in the total and readily releasable SV pools. The progressive decline in the total as well as readily releasable SV pools at the synapses may impair neurotransmission, contributing to INCL neuropathology.

## Discussion

In this study, we first demonstrated that under physiological conditions, PPT1 is detectable in the presynaptic compartment (i.e., synaptosomes and SVs). We also demonstrated that PPT1 deficiency causes persistent membrane sorting and retention of several SV proteins (i.e., VAMP2, SNAP25, syntaxin 1, SYTI, and GAD65), which are known to undergo palmitoylation. These proteins play critical roles in locally recycling the vesicle components fused with the presynaptic plasma membrane for neurotransmitter exocytosis and in regenerating fresh vesicles following exocytosis. Under normal conditions, the fresh vesicles generated replenish the readily releasable as well as the total SV pools at the synaptic terminals for further rounds of use. However, disproportionate and persistent membrane sorting and retention of VAMP2, SNAP25, SYTI, and GAD65 are likely to disrupt the recycling and regeneration of fresh vesicles, thus disrupting neurotransmission.

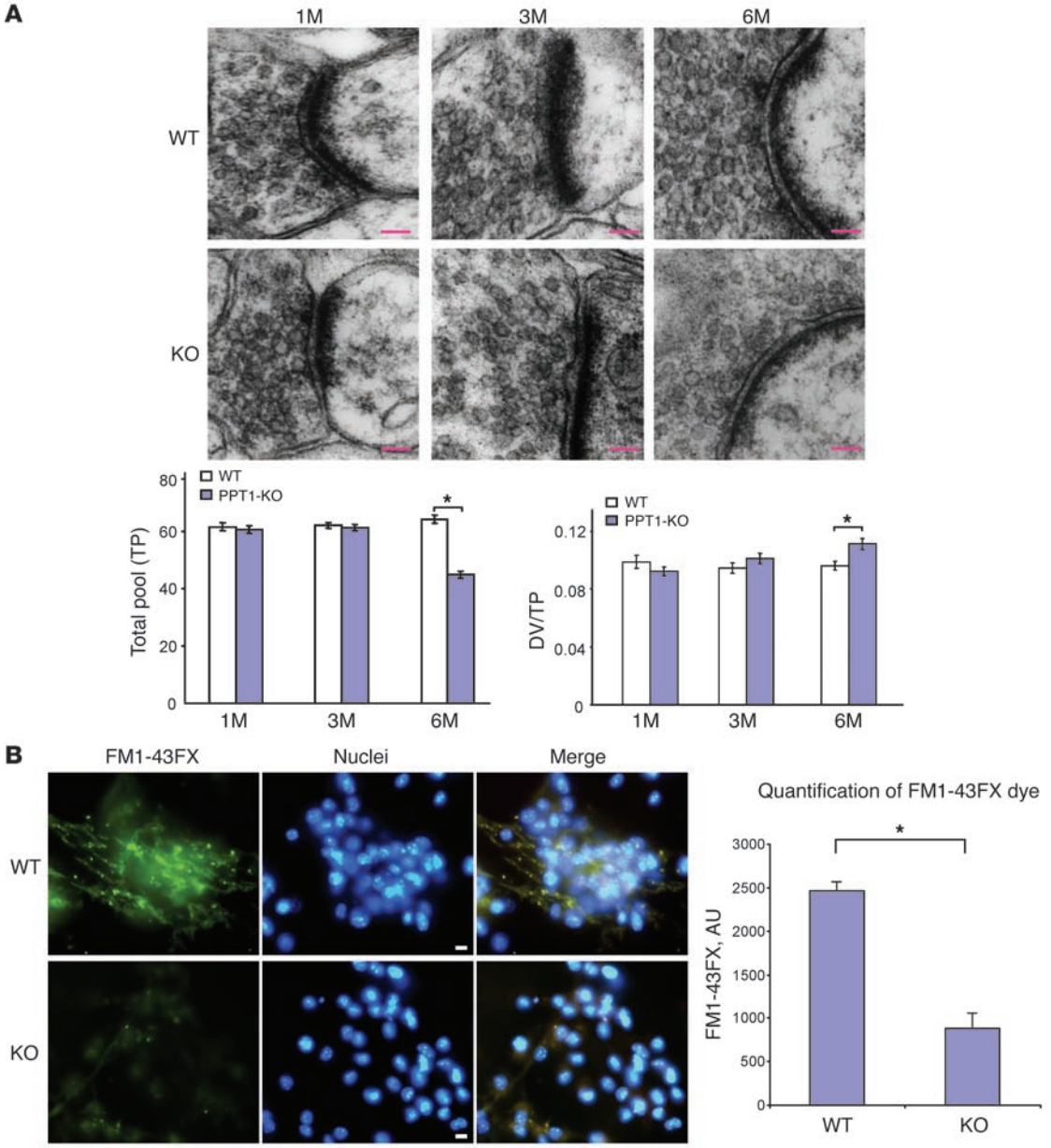


**Figure 6**
Analysis of SV pools in the WT and PPT1-KO mouse brains. (**A**) Cortical tissues from 1-, 3-, and 6-month-old WT and PPT1-KO mice were analyzed by transmission electron microscopy. Note a marked decline in the number of SVs in the 6-month-old PPT1-KO mice. Total vesicle numbers and ratio of docked vesicles to total vesicles are shown below the images. (**B**) The levels of readily releasable SV pools in cultured neurons from WT and PPT1-KO mice. Active (readily releasable) vesicles were detected by the release of styryl dye FM1-43FX (green) from the WT and PPT1-KO neurons. Nuclei were stained with DAPI. Scale bars: 20 μm. FM dye uptake quantification is shown on the right. *$P < 0.0001$. Data are mean ± SD ($n = 3$).

Our results clearly demonstrate that under physiological conditions, PPT1 immunoreactivity is localized in synaptosomes and SVs in addition to its expected presence in the lysosomes. These results were derived from analyzing the mouse brain tissues as well as the cultured neurons. The cultured neurons used in this study were not induced to overexpress PPT1, as reported previously (31–33), although our results are in agreement with those reports. As expected, we found that PPT1 immunoreactivity was undetectable in the PPT1-KO mouse brain and in cultured neurons differentiated from PPT1-deficient neurospheres. Thus, our results unambiguously demonstrate that PPT1 immunoreactivity is localized in the presynaptic compartment and rule out the possibility of a nonspecific distribution of PPT1 in extralysosomal organelles that may occur in induced overexpression models used in previous studies (31–33). How might a lysosomal enzyme such as PPT1 be present in extralysosomal compartments? Recently, it has been reported that at least a fraction of the freshly endocytosed vesicles during synaptic activity fuse with early endosomes (44), which may

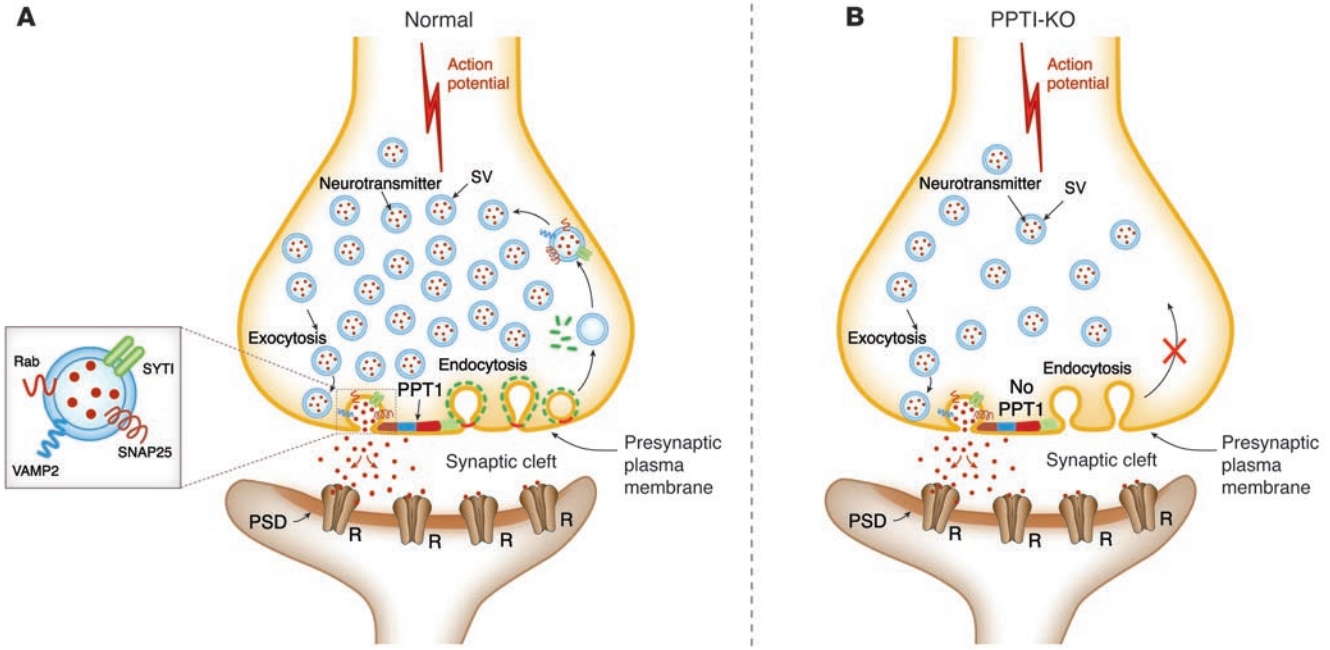


**Figure 7**

A model explaining how PPT1 deficiency may cause progressive decline the SV pool size. (**A**) Under normal circumstances, the SVs with their complement of *S*-acylated proteins dock on the presynaptic plasma membrane, fuse, and release neurotransmitters by exocytosis. The SV-associated proteins then undergo depalmitoylation by PPT1 detaching them from the membrane for recycling and regeneration of fresh vesicles by endocytosis. The newly generated SVs then reassociate with the recycled proteins, fill up with neurotransmitters, and restore the SV pool size. (**B**) PPT1 deficiency does not adversely affect SV fusion with the presynaptic plasma membrane. However, the lack of PPT1 prevents detachment of the palmitoylated SV proteins from membranes, and regeneration of fresh SVs is impaired. A gradual decline in the number of freshly regenerated SVs ultimately causes progressive reduction in the SV pool size, impairing neurotransmission. R, receptor.

contain lysosomal enzymes including PPT1. Consistent with this notion, a recent study (45) detected LAMP1, a lysosomal protein, in morphologically and biochemically homogenous SV preparations. Taken together, these results suggest that lysosomal proteins may be found in SVs and make it highly unlikely that PPT1 immunoreactivity, which we (in the present study) and others (31–33) have detected in synaptosomes and/or SVs, could be an artifact.

In the nerve terminals, SVs continuously recycle locally within the presynaptic compartment (16, 46), and these vesicles represent a model organelle for elucidating the mechanism(s) of membrane trafficking (15). Recently, by combining biophysical and proteomic approaches, it has been found that several proteins critical for exocytosis, recycling and regeneration of vesicles, including VAMP2, SNAP25, SYTI, and GAD65, are relatively abundant in SVs (47). These proteins undergo palmitoylation facilitating membrane anchorage and fusion with the presynaptic membrane, required for SV exocytosis. SNARE proteins VAMP2 and SNAP25 as well as the non-SNARE protein GAD65 undergo palmitoylation. Recent reports indicate that an intact palmitoylation-depalmitoylation cycle is critical for regulating the localization of proteins such as HRas and NRas (48, 49) and GAD65 (50) between Golgi membranes and the cytosolic face of the plasma membrane. Thus, the lack of depalmitoylation in INCL and in the PPT1-KO mice may disrupt the trafficking of these proteins, provided of course that these proteins are PPT1 substrates. Interestingly, although SNAP25 and SYTI have been reported to be stably associated with palmitate in PC-12 cells (51), our results from the brain tissues of INCL patients and those of the PPT1-KO mice seem to suggest that these proteins may be dynamically palmitoylated in vivo. Since all *S*-acylated proteins must undergo depalmitoylation to detach from the membrane, which is required for recycling, PPT1 deficiency may cause the SV proteins to remain membrane bound, thereby impairing SV recycling. Indeed, our results show an abnormal pattern of membrane sorting and persistent retention of these proteins in the PPT1-KO neurons and in synaptosomes purified from the brain tissues of the PPT1-KO mice. The apparent abnormal pattern of membrane association of syntaxin 1 is similar to that of SNAP25. This pattern may arise due to the fact that syntaxin 1 interacts with SNAP25 (23, 47), which undergoes palmitoylation, and thereby follows the pattern of SNAP25 even though syntaxin 1 itself is not a palmitoylated protein. Consistent with this notion, we found that immunoprecipitation of the lysates of cultured WT and PPT1-KO neurons using syntaxin 1 antibody (see Supplemental Methods) coprecipitate both syntaxin 1 and SNAP25 and that the levels of both proteins in the lysates of the PPT1-KO neurons are lower than those in WT neurons (Supplemental Figure 5A). However, while PPT1 deficiency causes abnormal membrane sorting and retention of SV proteins in the presynaptic compartment, it does not appear to affect the palmitoylated proteins in the postsynaptic compartment. This notion is supported by the fact that the postsynaptic density protein 95, which also undergoes palmitoylation (28), is distributed equally among the soluble and membrane fractions of PPT1-deficient cultured neurons, a pattern virtually identical to that found in the lysates of WT neurons (Supplemental Figure 5B). These results suggest that while PPT1 may depalmitoylate *S*-acylated proteins in

the presynaptic compartment, it may not affect those in the postsynaptic compartment. This conclusion is further supported by the fact that in immunoelectron microscopic analyses of the neurons, PPT1 immunoreactivity is not detectable in the postsynaptic compartment (data not shown).

How might lack of PPT1 disrupt the regeneration of fresh SVs following exocytosis? Recent reports indicate that upon exocytosis, SV proteins are released into the presynaptic compartment and retrieved by compensatory endocytosis (52). However, since palmitoylation of several SV proteins is critical for the attachment and fusion of the SVs to the presynaptic plasma membrane, PPT1 deficiency may prevent or drastically slow the recycling of these proteins due to the inability of these *S*-acylated proteins to detach from the presynaptic membrane, as explained in the graphic model in Figure 7. Further, disruption of SV protein recycling, due to the persistent membrane association, may impair the reassembly of SV constituents, thereby preventing the regeneration of fresh vesicles, and cause progressive reduction in the SV pool size at the synaptic terminal. Indeed, the results of our confocal and electron microscopic analyses show a progressive decline in the readily releasable and the total SV pool size in the PPT1-deficient neurons. Consistent with these findings, it has been recently reported that cultured cortical neurons from the PPT1-KO mice show a progressive reduction in the SV pool size at the synapses, which results in decreased frequency of miniature synaptic currents (53). Moreover, a recent gain-of-function modifier screen in *Drosophila* has identified modifier genes that link PPT1 function with SV cycling, endosomal trafficking, synaptic development and activity-dependent remodeling of the synapse (54). Indeed, alteration of synaptic functions such as SV cycling and endocytosis may explain the progressive decline in the SV pool size, as has also been reported in the mouse model of Huntington disease (55, 56). Our demonstration that lack of PPT1 causes abnormal membrane sorting and persistent membrane association of the SV proteins VAMP2, SNAP25, syntaxin 1, SYTI, and GAD65 is consistent with the notion that PPT1 is an integral part of the SV recycling and regeneration process and that its absence leads to abnormal neurotransmission, contributing to INCL neuropathology.

While in the present study we uncovered one of the possible mechanisms by which the lack of PPT1 may cause progressive decline in the SV pool size, other factors may also contribute to this outcome. For instance, loss-of-function mutations in several genes including synapsin (57, 58), β-catenin (59), dynamin (60), endophilin, and synaptojanin (61) may cause a decline in SV pool at the synaptic terminals. Moreover, recently it has been demonstrated that dynamin 1 plays pivotal roles in the endocytosis of SVs (62) and inhibition of dynamin by dynasore completely blocks compensatory endocytosis of the SVs (63). Although, it is not clear whether the neuronal isoform of dynamin, dynamin 1, is palmitoylated, our analysis of the amino acid sequence of dynamin 1, using an algorithm (CSS Palm; ref. 64), show that Cys960 and Cys956 in human and mouse dynamin 1, respectively, are potential palmitoylation sites. Our ongoing studies on the analysis of dynamin 1 in postmortem brain tissues from INCL patients and those from the PPT1-KO mice may provide experimental evidence as to whether this prediction is correct and whether PPT1 deficiency impairs dynamin 1 activity and contributes to the progressive decline of the SV pool size in the PPT1-KO mice.

## Methods

*PPT1-KO mice and genotyping.* PPT1-KO mice (a generous gift from S.L. Hofmann, University of Texas Southwestern Medical Center at Dallas, Dallas, Texas, USA) were generated by gene targeting in ES cells as previously described (33). These mice were backcrossed to obtain isogenic C57 genetic background in the laboratory of M.S. Sands (Washington University School of Medicine, St. Louis, Missouri, USA), who kindly provided the mating pair that established our colony of these mice. All mice were maintained and housed in a specific pathogen–free facility, and animal procedures were carried out in accordance with institutional guidelines after the National Institute of Child Health and Human Development (NICHD) Animal Care and Use Committee approved the study protocol.

*Postmortem brain tissues from control and INCL patients.* Brain autopsy tissue samples from a patient with INCL were obtained from the Human Brain and Spinal Fluid Resource Center at the VA West Los Angeles Healthcare Center (Los Angeles, California, USA). We also obtained postmortem control brain tissue samples from the Brain and Tissue Bank for Developmental Disorders at the University of Maryland (Baltimore, Maryland, USA). These tissues were obtained under an approved protocol by the NICHD Institutional Review Board. A sister of this patient, who also died from INCL, was a compound heterozygote for PPT1 mutations (del 398T in exon 4 and C451T in exon 5) (65). Since INCL is an autosomal recessive disease, we assume that the patient was also a compound heterozygote for the same PPT1 mutations.

*Cortical neuron culture.* Primary cortical neurons were cultured as previously described (66), with minor modifications. Briefly, cerebral cortices were isolated from 1- to 2-day-old homozygous PPT1-KO and WT mice and dissociated in 0.25% trypsin by trituration. The dissociated cells were cultured in either polylysine-coated slide chambers (Nunc) or in petri dishes using neurobasal medium (Invitrogen) supplemented with 10% heat-inactivated fetal bovine serum, 300 μM glutamine, 2% B27, 25 μM β-mercaptoethanol, and antibiotics. The medium was changed 24 h after plating the cells, and 3 days after plating, 50% of the medium was changed with fresh medium. Subsequently, medium was changed every 3–4 days.

*Neurosphere culture and neuron differentiation in vitro.* Mouse neurospheres were isolated from the brains of 15-day-old fetuses of PPT1-KO and WT littermates. The cells were cultured in NeuroCult NSC Basal Medium (StemCell Technologies) containing NeuroCult NSC proliferation supplements and human epidermal growth factor (final concentration of 20 ng/ml). To achieve neuronal differentiation, the proliferating neurospheres were cultured in NeuroCult NSC Basal Medium containing Neurocult NSC differentiation supplements. The cultures were incubated at 37°C under an atmosphere of 5% $CO_2$ and 95% air.

*Preparation of purified synaptosomal fraction from cerebral cortex.* Purified synaptosomal fraction was prepared from cerebral cortex of PPT1-KO mice and their WT littermates, as previously described (67). Briefly, cortical tissues were homogenized in ice-cold buffered sucrose solution (320 mM sucrose/4 mM HEPES-NaOH buffer/1× protease inhibitor [Pierce Biotechnology], pH 7.3) and centrifuged at 1,000 *g* for 10 min at 4°C. The supernatant thus obtained was centrifuged at 17,000 *g* for 55 min at 4°C. The resulting pellet was then resuspended in buffered sucrose solution and layered on top of a discontinuous sucrose density gradient consisting of 0.8 M and 1.2 M sucrose solution. The gradient was centrifuged at 54,000 *g* for 90 min at 4°C, and the synaptosomal fraction was obtained at the interface between 0.8 M and 1.2 M sucrose layer. This fraction was then removed carefully, diluted with 10 volumes of ice-cold buffered sucrose solution, and centrifuged at 20,000 *g* for 15 min at 4°C. The resulting pellet thus obtained was referred to as the "purified synaptosomal fraction," from which the membrane fraction was prepared using Mem-PER Eukaryotic Protein Extraction Kit (Pierce Biotechnology) and used for western blot analysis.

*Western blot analyses*. The brain cortical tissues were homogenized in protein-extracting buffer (50 mM Tris-HCl, 150 mM NaCl, 0.25% SDS, 1 mM EDTA, and 1% NP-40) containing protease-inhibitor cocktails (Sigma-Aldrich). For the preparation of total lysates from cultured neurons differentiated from WT or PPT1-KO neurospheres, cells were homogenized in Phosphosafe extraction reagent (EMD Biosciences). Proteins from the soluble and the membrane fractions were prepared using Mem-PER Eukaryotic Membrane Protein Extraction Kit (Pierce Biotechnology). Total proteins (20 μg) from each sample were resolved by electrophoresis using 4%–15% SDS-polyacrylamide gels (Bio-Rad) under denaturing and reducing conditions. Proteins were then electrotransferred to nitrocellulose membrane (Bio-Rad). The membranes were blocked with 5% non-fat dry milk (Bio-Rad) and then subjected to immunoblot analysis using standard methods. The primary antibodies used in the present study were anti-VAMP2, anti-SNAP25, anti–NaK ATPase, anti-synaptophysin (Abcam), anti–syntaxin 1, anti-PPT1 (Santa Cruz Biotechnology Inc.), and anti–β-actin (US Biological). The secondary antibodies wee goat anti-rabbit IgG (Santa Cruz Biotechnology Inc.) and rabbit anti-mouse IgG (Santa Cruz Biotechnology Inc.). Chemiluminescence was detected using SuperSignal west pico luminol/enhancer solution (Pierce Biotechnology) according to the manufacturer's instructions. Densitometric analysis was performed by Quantity One software (Bio-Rad). Densitometric measurements of the protein bands were obtained from 3 independent gels and the results statistically analyzed by using the Student's *t* test. Error bars in the figures indicate standard deviation ($n = 3$).

*[$^3$H]-palmitate labeling of proteins and immunoprecipitation*. Cells were first incubated in NeuroCult medium containing fatty acid–free BSA for 3 h and then metabolically labeled with [$^3$H]–palmitic acid (specific activity 200 μCi/ml palmitate; Amersham Pharmacia Biotech) containing NeuroCult medium (StemCell Technologies) for 6 h. Labeled cells were washed twice with ice-cold PBS and further processed with Mem-PER Eukaryotic Protein Extraction Kit (Pierce Biotechnology). For immunoprecipitation, the samples were then incubated with VAMP2 or SNAP25 antibodies (anti-rabbit, 1:100; Abcam) and anti-mouse GAD65 antibody (1:50) overnight at 4°C. After adding 100 μl protein A Sepharose beads (Amersham Pharmacia Biotech), samples were incubated for 1 h at 4°C. Immunoprecipitates were washed 3 times with buffer containing 50 mM Tris-HCl, pH 7.2, 1 mM EDTA, 1 mM EGTA, 150 mM NaCl, and 0.3% Triton X-100 and boiled in SDS-PAGE sample buffer (80 mM Tris, pH 6.8, 10% glycerol, 5% SDS, 150 mM dithiothreitol, 0.005% bromophenol blue) for 5 min. For autoradiography, protein samples were resolved by SDS-PAGE and dried using a vacuum dryer, gels were exposed to BAS-IIIs Imaging plate (Fuji) for 2 weeks, and the images were processed using the BAS-1500 Reader (Fuji) with the Image Reader version 1.4E and Image Gauge version 3.0 programs (Fuji).

*Confocal and fluorescent microscopic imaging*. For immunofluorescent microscopic detection, primary cultured PPT1-KO and WT mouse neurons were incubated at 37°C in an atmosphere of 5% of $CO_2$ and 95% air for 72 h on slide chambers (Nunc). The cells were washed 3 times with PBS, pH 7.6, and incubated 3.7% formaldehyde solution for 15 min at room temperature. The primary antibodies used in the present study were anti-LAMP1 and anti-PPT1 (Santa Cruz Biotechnology) and anti-synaptophysin, anti-VAMP2, and anti-SNAP25 (Abcam). The secondary antibodies used were Alexa Fluor 488–conjugated anti-goat, Alexa Fluor 555–conjugated anti-rat, Alexa Fluor 555–conjugated anti-rabbit, and Alexa Fluor 633–conjugated anti-rabbit (Invitrogen). Nuclei were stained with DAPI (Sigma-Aldrich). Fluorescence was visualized with the Zeiss LSM 510 Inverted Meta confocal microscope (Carl Zeiss), and the image was processed with the LSM image software (Carl Zeiss). To detect readily releasable (active) vesicles, PPT1-KO and WT mouse neurons differentiated from cultured neurospheres were incubated at 37°C in an atmosphere of 5% $CO_2$ and 95% air for 72 h on slide chambers (Nunc). To label active synapses, neurons were challenged by a hyperkalemic solution (60 mM KCl, 39 mM NaCl, 30 mM glucose, 25 mM HEPES, 2 mM $CaCl_2$, and 4 mM $MgCl_2$) containing 10 μM FM1-43FX [fixable version of *N*-(3-triethylammoniumpropyl)-4-(4-(dibutylamino)styryl) pyridinium dibromide] (Invitrogen) for 30–60 s, as previously described (65). Excess dye was removed with 7 rinses of 1 min each in external solution, 2 of which contained 1 mM Advasep7 (Sigma-Aldrich). Immediately after the rinses, neurons were fixed in 3.8% paraformaldehyde solution. Fluorescence was visualized with the Axioskop2 plus fluorescence microscope (Carl Zeiss), and the image was processed with the AxioVision 4.3 (Carl Zeiss). FM1-43FX dye uptake quantification was performed as previously described (68). FM dyes were measured and defined in arbitrary units. In each experiment, images were acquired using identical settings and the same threshold was used for all groups. All experiments were performed at 6 different locations and repeated 3 times with the same effect.

*Transmission electron microscopy*. The brain tissues were fixed in 2.5% glutaraldehyde in sodium phosphate buffer for 2 h at room temperature. The tissues were then washed with Millonig's phosphate buffer once and kept in the same buffer at 4°C until final processing. Lead citrate and uranyl acetate were used to stain the ultra-thin sections, which were then examined with a LEO 912 electron microscope (JFE Enterprises). Quantitation of the SVs was performed in cortical neurons as described previously (69). Briefly, only synapses with well-defined postsynaptic density were included in counting the SVs. Vesicles touching the membrane and those were within 1 vesicle diameter from the membrane were counted as docked vesicles. SVs were counted in at least 35 synapses for each genotype, and the results are expressed as the mean number of vesicles/μm$^2$ of synaptic surface ± SD. The data were analyzed by Student's *t* test.

*Immunoelectron microscopic analysis*. Adult WT and PPT1-KO mice were perfused fixed with 4% paraformaldehyde plus 0.1% glutaraldehyde in PBS. The brains were removed from the skull and further fixed in the same perfusion fixative for 1 h at 4°C. After fixation, the brains were put into PBS and 80-μm sections were cut at 4°C (Pelco 100 Vibratome Sectioning System; Ted Pella Inc.). The sections were then rinsed in PBS. At this point, the variable-wattage Pelco BioWave Pro microwave oven (Ted Pella Inc.) was used to incubate antibodies and process sections for electron microscopy. Before incubating sections, they were first treated in a 0.01-M citrate buffer, pH 6.0, (antigen retrieval step) for approximately 5 min until a temperature of 30°C was attained. Sections were then washed in blocking buffer for 2 min at a temperature of 30°C (1% BSA, 3% normal goat serum, 0.5% Triton X-100, and 1% fish gelatin in PBS) and then incubated in the primary antibody (1:50 in working buffer of 0.1% BSA, 0.3% normal goat serum, 0.1% Triton X-100, and 0.1% fish gelatin in PBS) for 16 min at 30°C. Next, the tissue was rinsed in working buffer for 2 min at 30°C and incubated with conjugated gold secondary antibody (rabbit anti-goat IgG, EM grade 10 nm conjugated gold; Electron Microscopy Sciences) diluted 1:50 in working buffer for 16 min at 30°C. After incubation, the sections were rinsed in PBS. Negative controls (minus primary antibody) were performed in parallel to the experimental sections, in which only the secondary antibody was used. The tissue sections were postfixed in 1% osmium tetroxide (Electron Microscopy Sciences) made in PBS for 10 min at 30°C. Next, sections were rinsed once in double-distilled water for 10 min (outside of microwave oven), en-blocked for 2 min at 30°C in 1% uranyl acetate (Polysciences Inc.) made in double-distilled water, and dehydrated in increasing concentrations of ethanol for 40 s each at a temperature of 50°C. The tissue sections were then infiltrated into increasing concentrations of Embed-812 (Electron Microscopy Sciences) epoxy via propylene oxide. The sections were embedded and polymerized in 100%

resin for 16 h in a lab oven set at 60°C. Thin sections were prepared on a Reichert-Jung Ultracut-E ultramicrotome (95-nm thick). The grids were post-stained with uranyl acetate and lead citrate and examined in a JEOL 1010 transmission electron microscope operating at 80 kV.

*Transfection of cells with cDNA constructs*. Cultured PPT1-KO astrocytes were transfected with their respective cDNA constructs using Lipofectamine 2000 reagent (Invitrogen) according to the manufacturer's protocol. The plasmids used for transfection were prepared using a Plasmid Midi Kit (QIAGEN). The consistency between plasmid preparations was monitored by determining the concentration of plasmids by both spectrophotometry and agarose gel electrophoresis. The cDNA clones used in the present study were VAMP2, PPT1 (Origene), and GAD65 (Open Biosystems).

## Acknowledgments

We thank J.Y. Chou, I. Owens, J.T. Russell, and S.W. Levin for critical review of the manuscript and helpful suggestions. The statistical analysis of the SV data by H. Wei is gratefully acknowledged. We are also grateful to V. Schram (Microscopy and Imaging Core, National Institute of Child Health and Human Development [NICHD]) for confocal microscopy and L. Holtzclaw (Section on Cellular and Synaptic Physiology, NICHD) for her expert assistance with the perfusion of the mouse brain. Brain autopsy tissue samples were obtained from the Human Brain and Spinal Fluid Resource Center at the VA West Los Angeles Healthcare Center (Los Angeles, California, USA), which is sponsored by the National Institute of Neurological Disorders and Stroke/National Institute of Mental Health, National Multiple Sciences Society, and the Department of Veterans Affairs. This research was supported in whole by the Intramural Research Program of the NICHD, NIH.

Received for publication August 2, 2007, and accepted in revised form July 9, 2008.

Address correspondence to: Anil B. Mukherjee, NIH, Building 10, Room 9D42, 10 Center Drive, Bethesda, Maryland 20892-1830, USA. Phone: (301) 496-7213; Fax: (301) 402-6632; E-mail: mukherja@exchange.nih.gov.

Sung-Jo Kim, Zhongjian Zhang, and Chinmoy Sarkar contributed equally to this work.

1. Linder, M.E., and Deschenes, R.J. 2007. Palmitoylation: policing protein stability and traffic. *Nat. Rev. Mol. Cell Biol.* **8**:74–84.
2. Resh, M.D. 2006. Palmitoylation of ligands, receptors and intracellular signaling molecules. *Sci. STKE.* **359**:1–14.
3. Smotrys, J.E., and Linder, M.E. 2004. Palmitoylation of intracellular signaling proteins: regulation and function. *Annu. Rev. Biochem.* **73**:559–587.
4. Fukuta, M., Fukuta, F., Adesnik, H., Nicoll, R.A., and Bredt, D.S. 2004. Identification of PSD-95 palmitoylating enzymes. *Neuron.* **44**:987–996.
5. Camp, L.A., and Hofmann, S.L. 1993. Purification and properties of a palmitoyl-protein thioesterase that cleaves palmitate from H-Ras. *J. Biol. Chem.* **268**:22566–22574.
6. Camp, L.A., Verkruyse, L.A., Afendis, S.J., Slaughter, C.A., and Hofmann, S.L. 1994. Molecular cloning and expression of palmitoyl-protein thioesterase. *J. Biol. Chem.* **269**:23212–23219.
7. Vesa, J., et al. 1995. Mutations in the palmitoyl protein thioesterase gene causing infantile neuronal ceroid lipofuscinosis. *Nature.* **376**:584–587.
8. Hobert, J.A., and Dawson, G. 2006. Neuronal ceroid lipofuscinoses therapeutic strategies: past, present and future. *Biochim. Biophys. Acta.* **1762**:945–953.
9. Haltia M. 2006. The neuronal ceroid-lipofuscinoses: from past to present. *Biochim. Biophys. Acta.* **1762**:850–856.
10. Goebel, H.H., and Wisniewski, K.E. 2004. Current state of clinical and morphological features in human NCL. *Brain Pathol.* **14**:61–69.
11. Mole, S.E. 2004. The genetic spectrum of human neuronal ceroid-lipofuscinoses. *Brain Pathol.* **14**:70–76.
12. Hofmann, S.L., and Peltonen, L. 2001. The neuronal ceroid lipofuscinoses. In *The metabolic & molecular bases of inherited disease.* 8th edition. C.R. Scriver, et al., editors. McGraw-Hill. New York, New York, USA. 3877–3894.
13. Krauss, G.L., and Mathews, G.C. 2003. Similarities in mechanisms and treatments for epileptic and nonepileptic myoclonus. *Epilepsy Currents.* **3**:19–21.
14. De Camilli, P. 2004-2005. Molecular mechanisms in membrane traffic at the neuronal synapse: role of protein-lipid interactions. *Harvey Lect.* **100**:1–28.
15. Sudhof, T.C. 2004. The synaptic vesicle cycle. *Annu. Rev. Neurosci.* **27**:509–547.
16. Ryan, T.A. 2006. A pre-synaptic to-do list for coupling exocytosis to endocytosis. *Curr. Opin. Cell Biol.* **18**:416–421.
17. Murthy, V.N., and DeCamilli, P. 2003. Cell biology of the presynaptic terminal. *Annu. Rev. Neurosci.* **26**:701–728.
18. Jahn, R., and Sudhof, T.C. 1994. Synaptic vesicles and exocytosis. *Annu. Rev. Neurosci.* **17**:219–246.
19. Sollner, T., et al. 1993. SNAP receptors implicated in vesicle targeting and fusion. *Nature.* **362**:318–324.
20. Weber, T., et al. 1998. SNAREpins: minimal machinery for membrane fusion. *Cell.* **92**:759–772.
21. Veit, M., Becher, A., and Ahnert-Hilger, G. 2000. Synaptobrevin 2 is palmitoylated in synaptic vesicles prepared from adult, but not from embryonic brain. *Mol Cell Neurosci.* **15**:408–416.
22. Gonzalo, S., and Linder, M.E. 1998. SNAP-25 palmitoylation and plasma membrane targeting require a functional secretary pathway. *Mol. Biol. Cell.* **9**:585–597.
23. Fasshauer, D., and Margittai, M. 2004. A transient N-terminal interaction of SNAP-25 and syntaxin nucleates SNARE assembly. *J. Biol. Chem.* **279**:7613–7621.
24. Kang, R., et al. 2004. Presynaptic trafficking of synaptotagmin I is regulated by protein palmitoylation. *J. Biol. Chem.* **279**:50524–50536.
25. Christagau, S., et al. 1992. Membrane anchoring of the autoantigen GAD65 to microvesicles in pancreatic b-cells by palmitoylation in the NH2-terminal domain. *J. Cell Biol.* **118**:309–320.
26. Kanaani, J., et al. 2002. A combination of three distinct trafficking signals mediates axonal targeting and presynaptic clustering of GAD65. *J. Cell Biol.* **158**:1229–1238.
27. Kanaani, J., Diacovo, M.J., El-Husseini, Ael-D., Bredt, D.S., and Baekkeskov, S. 2004. Palmitoylation controls trafficking of GAD65 from Golgi membranes to axon-specific endosomes and a Rab5a-dependent pathway to presynaptic clusters. *J. Cell Sci.* **117**:2001–2013.
28. El-Husseini, Ael-D., et al. 2002. Synaptic strength regulated by palmitate cycling on PSD-95. *Cell.* **108**:849–863.
29. Hellsten, E., Vesa, J., Olkkonen, V.M., Jalanko, A., and Peltonen, L. 1996. Human palmitoyl protein thioesterase: evidence for lysosomal targeting of the enzyme and disturbed cellular routing in infantile neuronal ceroid lipofuscinosis. *EMBO J.* **15**:5240–5245.
30. Soyombo, A.A., and Hofmann, S.L. 1997. Molecular cloning and expression of palmitoyl-protein thioesterase 2 (PPT2), a homolog of lysosomal palmitoyl-protein thioesterase with a distinct substrate specificity. *J. Biol. Chem.* **272**:27456–27463.
31. Ahtiainen, L., Van Diggelen, O.P., Jalanko, A., and Kopra, O. 2003. Palmitoyl protein thioesterase 1 is targeted to the axons in neurons. *J. Comp. Neurol.* **455**:368–377.
32. Lehtovirta, M., et al. 2001. Palmitoyl protein thioesterase (PPT) localizes into synaptosomes and synaptic vesicles in neurons: implications for infantile neuronal ceroid lipofuscinosis (INCL). *Hum. Mol. Genet.* **10**:69–75.
33. Heinonen, O., et al. 2000. Expression of Palmitoyl protein thioesterase in neurons. *Mol. Genet. Metab.* **69**:123–129.
34. Gupta, P., et al. 2001. Disruption of PPT1 or PPT2 causes neuronal ceroid lipofuscinosis in knockout mice. *Proc. Natl. Acad. Sci. U. S. A.* **98**:13566–13571.
35. Bible, E., Gupta, P., Hofmann, S.L., and Cooper, J.D. 2004. Regional and cellular neuropathology in the palmitoyl protein thioesterase-1 null mutant mouse model of infantile neuronal ceroid lipofuscinosis. *Neurobiol. Dis.* **16**:346–359.
36. Ungar, D., and Hughson, F.M. 2003. SNARE protein structure and function. *Annu. Rev. Cell Dev. Biol.* **19**:493–517.
37. Pobbati, A.V., Stein, A., and Fasshauer, D. 2006. N- to C-terminal SNARE complex assembly promotes rapid membrane fusion. *Science.* **313**:673–676.
38. Fernandez-Alfonso, T., Kwan, R., and Ryan, T.A. 2006. Synaptic vesicles interchange their membrane proteins with a large surface reservoir during recycling. *Neuron.* **51**:179–186.
39. Deak, F., Schoch, S., Liu, X., Sudhof, T.C., and Lavalali, E.T. 2004. Synaptobrevin is essential for fast synaptic-vesicle endocytosis. *Nat Cell Biol.* **6**:1102–1108.
40. Schweizer, F.E., and Ryan, T.A. 2006. The synaptic vesicle:cycle of exocytosis and endocytosis. *Curr. Opin. Neurobiol.* **16**:298–304.
41. Sorensen, J.B. 2005. SNARE complexes prepare for membrane fusion. *Trends Neurosci.* **28**:453–455.
42. Kraszewski, K., et al. 1995. Synaptic vesicle dynamics in living hippocampal neurons visualized with CY3-conjugated antibodies directed against the luminal domains of synaptotagmin. *J. Neurosci.* **15**:4328–4342.
43. Betz, W.J., Mao, F., and Smith, C.B. 1996. Imaging exocytosis and endocytosis. *Curr. Opin. Neurobiol.* **6**:365–371.
44. Rizzoli, S.O., et al. 2006. Evidence for early endosome-like fusion of recently endocytosed synaptic vesicles. *Traffic.* **7**:1163–1176.
45. Takamori, S., et al. 2006. Molecular anatomy of a

trafficking organelle. *Cell.* **127**:831–846.
46. Zakharenko, S., Chang, S., O'Donoghue, M., and Popov, S.V. 1999. Neurotransmitter secretion along growing nerve processes: comparison with synaptic vesicle exocytosis. *J. Cell Biol.* **144**:507–518.
47. An, S.J., and Almers, W. 2004. Tracking SNARE complex formation in live endocrine cells. *Science.* **306**:1042–1046.
48. Rocks, O., et al. 2005. An acylation cycle regulates localization and activity of palmitoylated ras isoforms. *Science.* **307**:1746–1752.
49. Goodwin, J.S., et al. 2005. Depalmitoylated Ras traffics to and from the Golgi complex via a nonvesicular pathway. *J. Cell Biol.* **170**:261–272.
50. Kanaani, J., et al. 2008. A palmitoylation cycle dynamically regulates partitioning of the GABA-synthesizing enzyme GAD65 between ER–Golgi and post–Golgi membranes. *J. Cell. Sci.* **121**:437–449.
51. Heindel, U., Schmidt, M.F.G., and Veit, M. 2003. Palmitoylation sites and processing of synaptotagmin I, the putative calcium sensor for neurosecretion. *FEBS Lett.* **544**:57–62.
52. Wienisch, M., and Klingauf, J. 2006. Vesicular proteins exocytosed and subsequently retrieved by compensatory endocytosis are nonidentical. *Nat. Neurosci.* **9**:1019–1027.
53. Virmani, T., Gupta, P., Liu, X., Kavalali, E.T., and Hofmann, S.L. 2005. Progressively reduced synaptic vesicle pool size in cultured neurons derived from neuronal ceroid lipofuscinosis-1 knockout mice. *Neurobiol. Dis.* **20**:314–323.
54. Buff, H., Smith, A.C., and Korey, C.A. 2007. Genetic modifiers of Drosophila palmitoyl-protein thioesterase 1-induced degeneration. *Genetics.* **176**:209–220.
55. Li, J.Y., Plomann, M., and Brundin, P. 2003. Huntington's disease: A synaptopathy? *Trends Mol. Med.* **9**:414–420.
56. Smith, R., Brundin, P., and Li, J.Y. 2005. Synaptic dysfunction in Huntington's disease: a new perspective. *Cell. Mol. Life Sci.* **62**:1901–1912.
57. Rosahl, T.W., et al. 1993. Short-term synaptic plasticity is altered in mice lacking synapsin I. *Cell.* **75**:661–670.
58. Pieribone, V.A., et al. 1995. Distinct pools of synaptic vesicles in neurotransmitter release. *Nature.* **375**:493–497.
59. Bamji, S.X., et al. 2003. Role of beta-catenin in synaptic vesicle localization and presynaptic assembly. *Neuron.* **40**:719–731.
60. Hinshaw, J.E. 2000. Dynamin and its role in membrane fusion. *Annu. Rev. Cell Dev. Biol.* **16**:483–519.
61. Schuske, K.R., et al. 2003. Endophilin is required for synaptic vesicle endocytosis by localizing synaptojanin. *Neuron.* **40**:749–762.
62. Ferguson, S.M., et al. 2007. A selective activity-dependent requirement for dynamin 1 in synaptic vesicle endocytosis. *Science.* **316**:570–574.
63. Newton, A.J., Kirchhausen, T., and Murthy, V.N. 2006. Inhibition of dynamin completely blocks compensatory synaptic vesicle endocytosis. *Proc. Natl. Acad. Sci. U. S. A.* **103**:17955–17960.
64. Zhou, F., Xue, Y., Yao, X., and Xu, Y. 2006. CSS-Palm: Palmitoylation site prediction with a clustering and scoring strategy. *Bioinformatics.* **22**:894–896.
65. Kim, S.J., Zhang, Z., Hitomi, E., Lee, Y.C., and Mukherjee, A.B. 2006. Endoplasmic reticulum stress-induced caspase-4 activation mediates apoptosis and neurodegeneration in INCL. *Hum. Mol. Genet.* **15**:1826–1834.
66. Lesuisse, C., and Martin, L.J. 2002. Long-term culture of mouse cortical neurons as a model for neuronal development, aging, and death. *J. Neurobiol.* **51**:9–23.
67. Gray, E.G., and Whittaker, V.P. 1962. The isolation of nerve endings from brain: an electron-microscopic study of cell fragments derived by homogenization and centrifugation. *J. Anat.* **96**:79–88.
68. Leshchyns'ka, I., et al. 2006. The adhesion molecule CHL1 regulates incoating of clathrin-coated synaptic vesicles. *Neuron.* **52**:1011–1025.
69. Murphy, D.D., Rueter, S.M., Trojanowski, J.Q., and Lee, V. M.-Y. 2000. Synucleins are developmentally expressed, and a-synuclein regulates the size of presynaptic vesicular pool in primary hippocampal neurons. *J. Neurosci.* **20**: 3214–3220.